International Journal of Fracture **83:** 315–336, 1997.
© 1997 *Kluwer Academic Publishers. Printed in the Netherlands.*

Analysis of a row of elliptical inclusions in a plate using singular integral equations

NAO-AKI NODA[1] and TADATOSHI MATSUO[2]
[1]*Department of Mechanical Engineering, Kyusyu Institute of Technology, Kitakyusyu, Japan, 804*
[2]*Department of Mechanical Engineering, Fukushima National College of Technology, Iwaki, Japan, 970*

Received 9 July 1996; accepted in revised form 16 January 1997

Abstract. This paper deals with the interaction problem of a row of elliptical inclusions under uniaxial tension. The body force method is used to formulate the problem as a system of singular integral equations with Cauchy-type and logarithmic-type singularities, where the unknowns are densities of body forces distributed in infinite plates that have the same elastic constants as those of the matrix and inclusion. In order to satisfy the boundary conditions along the elliptical boundaries, eight kinds of fundamental density functions, proposed in a previous paper, are applied. In the analysis, the number, shape, and position of inclusions are varied systematically; after which the magnitude and position of the maximum stress are examined. For any fixed shape and size of inclusions, the maximum stress is shown to be linear with the reciprocal of the number of inclusions. The present method is found to yield rapidly converging numerical results for various geometrical conditions of inclusions.

Key words: stress concentration, elliptical inclusion, body force method, singular integral equation, a row of inclusions, interaction

1. Introduction

It is known that most engineering materials contain some defects in the form of cracks, voids, inclusions or second-phase particles. To evaluate the effect of defects on the strength of structures, it is important to know the stress concentration of elliptical inclusions in a plate under tension because they cover a wide variety of particular cases, such as line and circular defects. In previous research, one and two circular and elliptical inclusions were treated by several researchers [1–4], and was a row of elliptical holes recently solved by the problem of Isida and Igawa [5]. However, a row of elliptical inclusions has not been treated. The magnitude and location of the maximum stress of several inclusions vary slightly with a small change of the shape, size, location, or elastic constants of inclusions. In order to study this sensitivity, it is necessary to obtain the exact stress distribution along the interface between matrix and inclusions.

In preceding papers, the authors have considered elliptical holes and ellipsoidal cavities using singular integral equations of the body force method [6, 7]. This method can be applied to the analysis of various shapes and spacing of elliptical holes. In this paper the method will be applied to a row of elliptical inclusions in a plate under uniaxial tension using singular integral equations of the body force method. Then, the interaction effects will be discussed. The present method of analysis yields a smooth variation of stress distribution along the boundaries.

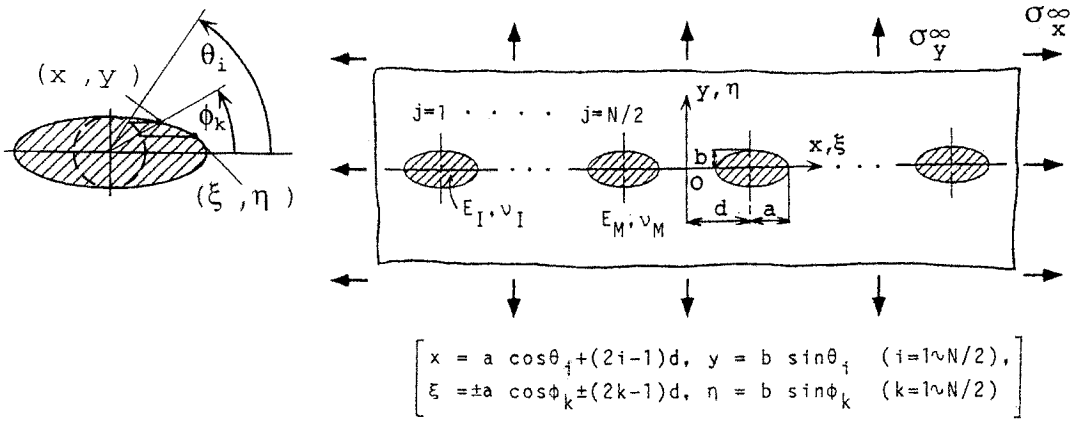

Figure 1. Periodic array of elliptical inclusions in an infinite plate (N is the number of inclusions).

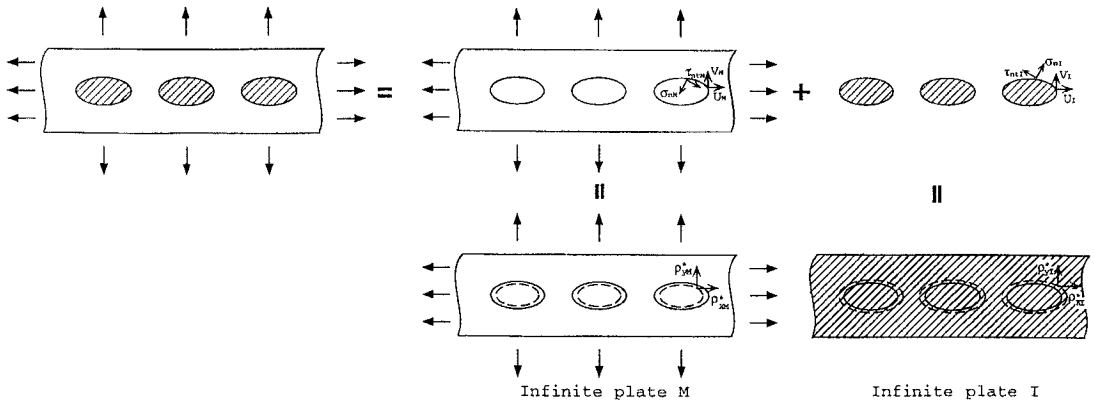

Figure 2. Formulation of the singular integral equation based on the body force method.

2. Method of analysis

2.1. Singular integral equations of the body force method

The method of analysis will be explained using the example of a row of elliptical inclusions in a plate subjected to tensile stresses at infinity, $\sigma_x^\infty, \sigma_y^\infty$ as shown in Figure 1. Here, the number of inclusions N is assumed to be an even one. However, the method is also applicable when an odd number is used. The body force method enables us to formulate the problem as a system of singular integral equations. Here, the fundamental solutions are the stress and displacement fields at an arbitrary point due to point forces acting symmetrically to the y-axis [8–10]. As shown in Figure 1, θ_i is a parametric angle of ellipse used to specify the point in question $(x, y) = (d + 2d(i-1) + a\cos\theta_i, b\sin\theta_i)$ $[i = 1, \ldots, N/2]$ and ϕ_k is also a parametric angle used to specify the point $(\xi, \eta) = (\pm d + 2d(k-1) + a\cos\phi_k, b\sin\phi_k)$ $[k = 1, \ldots, N/2]$ where the body force is applied.

Figure 2 illustrates the method of analysis. Consider two infinite plates. An infinite plate 'M' has the same elastic constants as the ones of the matrix, and an infinite plate 'I' has the same elastic constants as the ones of the inclusions. Denote $\sigma_{nM}, \tau_{ntM}, U_M, V_M$ as stresses and displacements which appear along the prospective boundaries of elliptical holes in the

infinite plate 'M'. In a similar way, denote $\sigma_{nI}, \tau_{ntI}, U_I, V_I$ as stresses and displacements which appear along the prospective boundaries of elliptical inclusions in the infinite plate 'I'. Then, Equations (1) and (2) enforce the boundary condition along the interface between 'M' and 'I', that is $\sigma_{nM} - \sigma_{nI} = 0, \tau_{ntM} - \tau_{ntI} = 0, U_M - U_I = 0, V_M - V_I = 0$.

$$
\begin{aligned}
&-(\tfrac{1}{2})\{\rho^*_{xM}(\theta_i)\cos\theta_{i0} + \rho^*_{yM}(\theta_i)\sin\theta_{i0}\} - (\tfrac{1}{2})\{\rho^*_{xI}(\theta_i)\cos\theta_{i0} + \rho^*_{yI}(\theta_i)\sin\theta_{i0}\} \\
&\quad + \sum_{k=1}^{N/2}\int_0^{2\pi} K^{Fx}_{nnM}(\phi_k,\theta_i)\rho^*_{xM}(\phi_k)\,\mathrm{d}s + \sum_{k=1}^{N/2}\int_0^{2\pi} K^{Fy}_{nnM}(\phi_k,\theta_i)\rho^*_{yM}(\phi_k)\,\mathrm{d}s \\
&\quad - \sum_{k=1}^{N/2}\int_0^{2\pi} K^{Fx}_{nnI}(\phi_k,\theta_i)\rho^*_{xI}(\phi_k)\,\mathrm{d}s - \sum_{k=1}^{N/2}\int_0^{2\pi} K^{Fy}_{nnI}(\phi_k,\theta_i)\rho^*_{yI}(\phi_k)\,\mathrm{d}s \\
&= -(\sigma^\infty_x\cos^2\theta_{i0} + \sigma^\infty_y\sin^2\theta_{i0}) \quad (i = 1,\ldots,N/2)
\end{aligned} \tag{1a}
$$

$$
\begin{aligned}
&-(\tfrac{1}{2})\{-\rho^*_{xM}(\theta_i)\sin\theta_{i0} + \rho^*_{yM}(\theta_i)\cos\theta_{i0}\} - (\tfrac{1}{2})\{-\rho^*_{xI}(\theta_i)\sin\theta_{i0} + \rho^*_{yI}(\theta_i)\cos\theta_{i0}\} \\
&\quad + \sum_{k=1}^{N/2}\int_0^{2\pi} K^{Fx}_{ntM}(\phi_k,\theta_i)\rho^*_{xM}(\phi_k)\,\mathrm{d}s + \sum_{k=1}^{N/2}\int_0^{2\pi} K^{Fy}_{ntM}(\phi_k,\theta_i)\rho^*_{yM}(\phi_k)\,\mathrm{d}s \\
&\quad - \sum_{k=1}^{N/2}\int_0^{2\pi} K^{Fx}_{ntI}(\phi_k,\theta_i)\rho^*_{xI}(\phi_k)\,\mathrm{d}s - \sum_{k=1}^{N/2}\int_0^{2\pi} K^{Fy}_{ntI}(\phi_k,\theta_i)\rho^*_{yI}(\phi_k)\,\mathrm{d}s \\
&= -(\sigma^\infty_y - \sigma^\infty_x)\sin\theta_{i0}\cos\theta_{i0} \quad (i = 1,\ldots,N/2)
\end{aligned} \tag{1b}
$$

$$
\begin{aligned}
&\sum_{k=1}^{N/2}\int_0^{2\pi} K^{Fx}_{uM}(\phi_k,\theta_i)\rho^*_{xM}(\phi_k)\,\mathrm{d}s + \sum_{k=1}^{N/2}\int_0^{2\pi} K^{Fy}_{uM}(\phi_k,\theta_i)\rho^*_{yM}(\phi_k)\,\mathrm{d}s \\
&\quad - \sum_{k=1}^{N/2}\int_0^{2\pi} K^{Fx}_{uI}(\phi_k,\theta_i)\rho^*_{xI}(\phi_k)\,\mathrm{d}s - \sum_{k=1}^{N/2}\int_0^{2\pi} K^{Fy}_{uI}(\phi_k,\theta_i)\rho^*_{yI}(\phi_k)\,\mathrm{d}s \\
&= -(\sigma^\infty_x - \nu_M\sigma^\infty_y)x/E_M \quad (i = 1,\ldots,N/2)
\end{aligned} \tag{2a}
$$

$$
\begin{aligned}
&\sum_{k=I}^{N/2}\int_0^{2\pi} K^{Fx}_{vM}(\phi_k,\theta_i)\rho^*_{xM}(\phi_k)\,\mathrm{d}s + \sum_{k=1}^{N/2}\int_0^{2\pi} K^{Fy}_{vM}(\phi_k,\theta_i)\rho^*_{yM}(\phi_k)\,\mathrm{d}s \\
&\quad - \sum_{k=1}^{N/2}\int_0^{2\pi} K^{Fx}_{vI}(\phi_k,\theta_i)\rho^*_{xI}(\phi_k)\,\mathrm{d}s - \sum_{k=1}^{N/2}\int_0^{2\pi} K^{Fy}_{vI}(\phi_k,\theta_i)\rho^*_{yI}(\phi_k)\,\mathrm{d}s \\
&= -(\sigma^\infty_y - \nu_M\sigma^\infty_x)y/E_M \quad (i = 1,\ldots,N/2)
\end{aligned} \tag{2b}
$$

where

$$-\mathrm{d}\xi = a\sin\phi_k\,\mathrm{d}\phi_k, \qquad \mathrm{d}\eta = b\cos\phi_k\,\mathrm{d}\phi_k, \qquad \mathrm{d}s = \sqrt{a^2\sin^2\phi_k + b^2\cos^2\phi_k}\,\mathrm{d}\phi_k. \tag{3}$$

In Equations (1) and (2), the unknown functions are the body force densities $\rho^*_{xM}(\phi_k)$, $\rho^*_{yM}(\phi_k)$ $(k = 1, \ldots, N/2)$ which are distributed in the infinite plate 'M', and the densities $\rho^*_{xI}(\phi_k)$, $\rho^*_{yI}(\phi_k)$ $(k = 1, \ldots, N/2)$ in the infinite plate 'I'. The notation θ_{i0} denotes the angle between the x-axis and the normal direction at the point (x, y). The summation $\Sigma_{k=1}^{N/2}$ means integrating the body force densities along the prospective kth boundaries of elliptical inclusions.

The first terms in Equation (1) represent the stresses which appear along the minus boundary that is infinitesimally apart from the initial boundary [8]. The notation, for example, $K^{Fx}_{nnM}(\phi_k, \theta_i)$ denotes the stress σ_n which appears at the elliptical boundaries when point forces are symmetrically acting at two different points on the boundaries. When $i = k$, Equation (1) has the Cauchy-type singularities and Equation (2) has logarithmic-type singularities. In this case, the integrations in Equation (1) should be interpreted as the principal values.

2.2. Numerical solution of the singular integral equations

The fundamental density functions $w_{x1}(\phi_k), \ldots, w_{x4}(\phi_k)$ distributed in the x-direction of the elliptical boundary and the ones $w_{y1}(\phi_k), \ldots, w_{y4}(\phi_k)$ distributed in the y-direction are defined as follows [6, 7].

$$\begin{aligned} w_{x1}(\phi_k) &= n_x(\phi_k)/\cos\phi_k, \\ w_{x2}(\phi_k) &= n_x(\phi_k)\tan\phi_k, \\ w_{x3}(\phi_k) &= n_x(\phi_k), \\ w_{x4}(\phi_k) &= n_x(\phi_k)\sin\phi_k, \end{aligned} \tag{4a}$$

$$\begin{aligned} w_{y1}(\phi_k) &= n_y(\phi_k)/\sin\phi_k, \\ w_{y2}(\phi_k) &= n_y(\phi_k), \\ w_{y3}(\phi_k) &= n_y(\phi_k)\cot\phi_k, \\ w_{y4}(\phi_k) &= n_y(\phi_k)\cos\phi_k, \end{aligned} \tag{4b}$$

where

$$\begin{aligned} n_x(\phi_k) &= \frac{b\cos\phi_k}{\sqrt{a^2\sin^2\phi_k + b^2\cos^2\phi_k}}, \\ n_y(\phi_k) &= \frac{a\sin\phi_k}{\sqrt{a^2\sin^2\phi_k + b^2\cos^2\phi_k}}. \end{aligned} \tag{5}$$

In this analysis, the unknown functions $\rho^*_{xM}(\phi_k), \rho^*_{yM}(\phi_k), \rho^*_{xI}(\phi_k), \rho^*_{yI}(\phi_k)$ $(k = 1, \ldots, N/2)$ are approximated by using (4a) and (4b). Here the weight functions $\rho_{x1}(\phi_k), \ldots, \rho_{y4}(\phi_k)$ $(k = 1, \ldots, N/2)$ are unknown functions defined in the range $0 \leqslant \phi_k \leqslant \pi/2$ and symmetric

with respect to the axis $\phi_k = 0$ and $\phi_k = \pi/2$. Since the problem has a symmetry with respect to the x-axis, only the functions $w_{x1}(\phi_k), w_{x3}(\phi_k), w_{y2}(\phi_k), w_{y4}(\phi_k)$ will be used. Then,

$$\rho^*_{xM}(\phi_k) = \rho_{x1M}(\phi_k)w_{x1}(\phi_k) + \rho_{x3M}(\phi_k)w_{x3}(\phi_k),$$

$$\rho^*_{yM}(\phi_k) = \rho_{y2M}(\phi_k)w_{y2}(\phi_k) + \rho_{y4M}(\phi_k)w_{y4}(\phi_k),$$

$$\rho^*_{xI}(\phi_k) = \rho_{x1I}(\phi_k)w_{x1}(\phi_k) + \rho_{x3I}(\phi_k)w_{x3}(\phi_k),$$

$$\rho^*_{yI}(\phi_k) = \rho_{y2I}(\phi_k)w_{y2}(\phi_k) + \rho_{y4I}(\phi_k)w_{y4}(\phi_k), \quad (k = 1, \ldots, N/2). \tag{6}$$

Using the expressions mentioned above, the singular integral equations are reduced to the following equations.

$$-(\tfrac{1}{2})[\{\rho_{x1M}(\theta_i)/\cos\theta_i + \rho_{x3M}(\theta_{i0})\}\cos^2\theta_{i0} + \{\rho_{y2M}(\theta_i) + \rho_{y4M}(\theta_i)\cos\theta_i\}\sin^2\theta_{i0}]$$

$$-(\tfrac{1}{2})[\{\rho_{x1I}(\theta_i)/\cos\theta_i + \rho_{x3I}(\theta_{i0})\}\cos^2\theta_{i0} + \{\rho_{y2I}(\theta_i) + \rho_{y4I}(\theta_i)\cos\theta_i\}\sin^2\theta_{i0}]$$

$$+\sum_{k=1}^{N/2}\int_0^{2\pi} K^{Fx}_{nnM}(\phi_k,\theta_i)\{\rho_{x1M}(\phi_k)/\cos\phi_k + \rho_{x3M}(\phi_k)\}b\cos\phi_k\,\mathrm{d}\phi_k$$

$$+\sum_{k=1}^{N/2}\int_0^{2\pi} K^{Fy}_{nnM}(\phi_k,\theta_i)\{\rho_{y2M}(\phi_k) + \rho_{y4M}(\phi_k)\cos\phi_k\}a\sin\phi_k\,\mathrm{d}\phi_k$$

$$-\sum_{k=1}^{N/2}\int_0^{2\pi} K^{Fx}_{nnI}(\phi_k,\theta_i)\{\rho_{x1I}(\phi_k)/\cos\phi_k + \rho_{x3I}(\phi_k)\}b\cos\phi_k\,\mathrm{d}\phi_k$$

$$-\sum_{k=1}^{N/2}\int_0^{2\pi} K^{Fy}_{nnI}(\phi_k,\theta_i)\{\rho_{y2I}(\phi_k) + \rho_{y4I}(\phi_k)\cos\phi_k\}a\sin\phi_k\,\mathrm{d}\phi_k$$

$$= -(\sigma^\infty_x\cos^2\theta_{i0} + \sigma^\infty_y\sin^2\theta_{i0}) \quad (i = 1, \ldots, N/2). \tag{7a}$$

$$-(\tfrac{1}{2})[-\{\rho_{x1M}(\theta_i)/\cos\theta_i + \rho_{x3M}(\theta_i)\} + \{\rho_{y2M}(\theta_i) + \rho_{y4M}(\theta_i)\cos\theta_i\}]\sin\theta_{i0}\cos\theta_{i0}$$

$$-(\tfrac{1}{2})[-\{\rho_{x1I}(\theta_i)/\cos\theta_i + \rho_{x3I}(\theta_i)\} + \{\rho_{y2I}(\theta_i) + \rho_{y4I}(\theta_i)\cos\theta_i\}]\sin\theta_{i0}\cos\theta_{i0}$$

$$+\sum_{k=1}^{N/2}\int_0^{2\pi} K^{Fx}_{ntM}(\phi_k,\theta_i)\{\rho_{x1M}(\phi_k)/\cos\phi_k + \rho_{x3M}(\phi_k)\}b\cos\phi_k\,\mathrm{d}\phi_k$$

$$+\sum_{k=1}^{N/2}\int_0^{2\pi} K^{Fy}_{ntM}(\phi_k,\theta_i)\{\rho_{y2M}(\phi_k) + \rho_{y4M}(\phi_k)\cos\phi_k\}a\sin\phi_k\,\mathrm{d}\phi_k$$

$$-\sum_{k=1}^{N/2}\int_0^{2\pi} K^{Fx}_{ntI}(\phi_k,\theta_i)\{\rho_{x1I}(\phi_k)/\cos\phi_k + \rho_{x3I}(\phi_k)\}b\cos\phi_k\,\mathrm{d}\phi_k$$

$$-\sum_{k=1}^{N/2}\int_0^{2\pi} K^{Fy}_{ntI}(\phi_k,\theta_i)\{\rho_{y2I}(\phi_k) + \rho_{y4I}(\phi_k)\cos\phi_k\}a\sin\phi_k\,\mathrm{d}\phi_k$$

$$= -(\sigma_y^\infty - \sigma_x^\infty)\sin\theta_{i0}\cos\theta_{i0} \quad (i = 1, \ldots, N/2) \tag{7b}$$

$$\begin{aligned}
&\sum_{k=1}^{N/2}\int_0^{2\pi} K_{uM}^{Fx}(\phi_k,\theta_i)\{\rho_{x1M}(\phi_k)/\cos\phi_k + \rho_{x3M}(\phi_k)\}b\cos\phi_k\,\mathrm{d}\phi_k \\
&\quad + \sum_{k=1}^{N/2}\int_0^{2\pi} K_{uM}^{Fy}(\phi_k,\theta_i)\{\rho_{y2M}(\phi_k) + \rho_{y4M}(\phi_k)\cos\phi_k\}a\sin\phi_k\,\mathrm{d}\phi_k \\
&\quad - \sum_{k=1}^{N/2}\int_0^{2\pi} K_{uI}^{Fx}(\phi_k,\theta_i)\{\rho_{x1I}(\phi_k)/\cos\phi_k + \rho_{x3I}(\phi_k)\}b\cos\phi_k\,\mathrm{d}\phi_k \\
&\quad - \sum_{k=1}^{N/2}\int_0^{2\pi} K_{uI}^{Fy}(\phi_k,\theta_i)\{\rho_{y2I}(\phi_k) + \rho_{y4I}(\phi_k)\cos\phi_k\}a\sin\phi_k\,\mathrm{d}\phi_k \\
&= -(\sigma_x^\infty - \nu_M\sigma_y^\infty)x/E_M \quad (i = 1, \ldots, N/2)
\end{aligned} \tag{8a}$$

$$\begin{aligned}
&\sum_{k=1}^{N/2}\int_0^{2\pi} K_{vM}^{Fx}(\phi_k,\theta_i)\{\rho_{x1M}(\phi_k)/\cos\phi_k + \rho_{x3M}(\phi_k)\}b\cos\phi_k\,\mathrm{d}\phi_k \\
&\quad + \sum_{k=1}^{N/2}\int_0^{2\pi} K_{vM}^{Fy}(\phi_k,\theta_i)\{\rho_{y2M}(\phi_k) + \rho_{y4M}(\phi_k)\cos\phi_k\}a\sin\phi_k\,\mathrm{d}\phi_k \\
&\quad - \sum_{k=1}^{N/2}\int_0^{2\pi} K_{vI}^{Fx}(\phi_k,\theta_i)\{\rho_{x1I}(\phi_k)/\cos\phi_k + \rho_{x3I}(\phi_k)\}b\cos\phi_k\,\mathrm{d}\phi_k \\
&\quad - \sum_{k=1}^{N/2}\int_0^{2\pi} K_{vI}^{Fy}(\phi_k,\theta_i)\{\rho_{y2I}(\phi_k) + \rho_{y4I}(\phi_k)\cos\phi_k\}a\sin\phi_k\,\mathrm{d}\phi_k \\
&= -(\sigma_y^\infty - \nu_M\sigma_x^\infty)y/E_M \quad (i = 1, \ldots, N/2).
\end{aligned} \tag{8b}$$

The unknown weight functions are approximated as continuous functions by using the following expressions.

$$\rho_{x1M}(\phi_k) = \sum_{n=1}^{M/2} a_{knM}t_n(\phi_k), \qquad \rho_{x3M}(\phi_k) = \sum_{n=1}^{M/2} b_{knM}t_n(\phi_k),$$

$$\rho_{y2M}(\phi_k) = \sum_{n=1}^{M/2} c_{knM}t_n(\phi_k), \qquad \rho_{y4M}(\phi_k) = \sum_{n=1}^{M/2} d_{knM}t_n(\phi_k),$$

$$\rho_{x1I}(\phi_k) = \sum_{n=1}^{M/2} a_{knI}t_n(\phi_k), \qquad \rho_{x3I}(\phi_k) = \sum_{n=1}^{M/2} b_{knI}t_n(\phi_k),$$

$$\rho_{y2I}(\phi_k) = \sum_{n=1}^{M/2} c_{knI} t_n(\phi_k),$$

$$\rho_{y4I}(\phi_k) = \sum_{n=1}^{M/2} d_{knI} t_n(\phi_k), \quad (k = 1, \ldots, N/2). \tag{9}$$

$$t_n(\phi_k) = \cos\{2(n-1)\phi_k\}. \tag{10}$$

Here, M is the number of collocation points in the range $0 \leqslant \theta_i \leqslant \pi$. Finally, the singular integral equations are reduced to the following algebraic equations, whose number of unknowns is $4M \times N/2$.

$$\sum_{k=1}^{N/2} \sum_{n=1}^{M/2} (a_{knM} A_{knM} + b_{knM} B_{knM} + c_{knM} C_{knM} + d_{knM} D_{knM} + a_{knI} A_{knI} + b_{knI} B_{knI} + c_{knI} C_{knI} + d_{knI} D_{knI}) = -(\sigma_x^\infty \cos^2 \theta_{i0} + \sigma_y^\infty \sin^2 \theta_{i0}) \quad (i = 1, \ldots, N/2) \tag{11a}$$

$$\sum_{k=1}^{N/2} \sum_{n=1}^{M/2} (a_{knM} E_{knM} + b_{knM} F_{knM} + c_{knM} G_{knM} + d_{knM} H_{knM} + a_{knI} E_{knI} + b_{knI} F_{knI} + c_{knI} G_{knI} + d_{knI} H_{knI}) = -(\sigma_y^\infty - \sigma_x^\infty) \sin \theta_{i0} \cos \theta_{i0} \quad (i = 1, \ldots, N/2) \tag{11b}$$

$$\sum_{k=1}^{N/2} \sum_{n=1}^{M/2} (a_{knM} I_{knM} + b_{knM} J_{knM} + c_{knM} K_{knM} + d_{knM} L_{knM} + a_{knI} I_{knI} + b_{knI} J_{knI} + c_{knI} K_{knI} + d_{knI} L_{knI}) = -(\sigma_x^\infty - \nu_M \sigma_y^\infty) x / E_M \quad (i = 1, \ldots, N/2) \tag{12a}$$

$$\sum_{k=1}^{N/2} \sum_{n=1}^{M/2} (a_{knM} M_{knM} + b_{knM} N_{knM} + c_{knM} O_{knM} + d_{knM} P_{knM} + a_{knI} M_{knI} + b_{knI} N_{knI} + c_{knI} O_{knI} + d_{knI} P_{knI}) = -(\sigma_y^\infty - \nu_M \sigma_x^\infty) y / E_M \quad (i = 1, \ldots, N/2) \tag{12b}$$

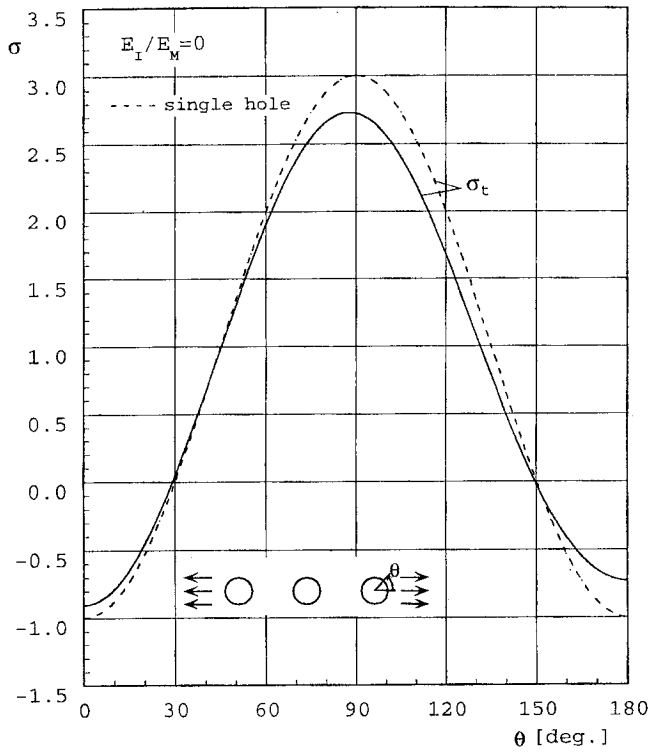

Figure 3. Stress distribution along the outer boundary for three circular inclusions. ($N = 3, a/b = 1, a/d = 0.4, \sigma_x^\infty = 1, \sigma_y^\infty = 0, E_I/E_M = 0$ in Figure 1)

$$A_{knM} = -(\tfrac{1}{2})t_n(\theta_i)\cos^2\theta_{i0}/\cos\theta_i + \int_0^{2\pi} K^{Fx}_{nnM}(\phi_k, \theta_i)t_n(\phi_k)b\,\mathrm{d}\phi_k$$
$$(i, k = 1, \ldots, N/2, n = 1, \ldots, M/2). \tag{13}$$

The unknown coefficients $a_{knM}, b_{knM}, c_{knM}, d_{knM}, a_{knI}, b_{knI}, c_{knI}, d_{knI}$ $(k = 1, \ldots, N/2, n = 1, \ldots, M/2)$ can be determined from boundary conditions at suitably chosen collocation points. Stresses at an arbitrary point can be expressed by using these coefficients and influence coefficients $A_{knM}, \ldots, P_{knI}$ $(k = 1, \ldots, N/2, n = 1, \ldots, M/2)$ which can be expressed in a similar form to Equation (13). The stresses along the elliptical inclusions are systematically obtained for various numbers, shapes and elastic moduli of inclusions.

3. Results and discussion

In the following calculations, plane strain conditions with Poisson's ratios $v_M = v_I = 0.3$ are assumed.

3.1. Convergence and boundary conditions

Table 1 shows a typical example of convergence of stresses $(\sigma_{nM}, \sigma_{tM}, \tau_{ntM}, \sigma_{nI}, \sigma_{tI}, \tau_{ntI})$ along the outermost boundary when the inclusion number $N = 5$, and $a/b = 1, a/d = 0.6, \sigma_x^\infty = 1, \sigma_y^\infty = 0, E_I/E_M = 0.5$. The results have convergence to five digits when $M =$

Table 1. Convergence of the interface stresses around the inclusion. ($N = 5, a/b = 1, a/d = 0.6, \sigma_x^\infty = 1, \sigma_y^\infty = 0, E_I/E_M = 0.5$ in Figure 1)

θ	M	σ_{tM}	σ_{tI}	σ_{nM}	σ_{nI}	τ_{ntM}	τ_{ntI}
	8	−0.26407	0.02279	0.72171	0.72177	0	0
0	12	−0.26412	0.02267	0.72166	0.72166	0	0
	16	−0.26412	0.02265	0.72164	0.72164	0	0
	8	0.45536	0.31838	0.42478	0.42478	−0.34616	−0.34617
40	12	0.45525	0.31846	0.42474	0.42474	−0.34613	−0.34613
	16	0.45523	0.31849	0.42473	0.42473	−0.34613	−0.34613
	8	1.39385	0.70413	0.03531	0.03531	−0.10530	−0.10532
80	12	1.39376	0.70439	0.03529	0.03529	−0.10529	−0.10529
	16	1.39376	0.70440	0.03528	0.03528	−0.10528	−0.10528
	8	1.42990	0.71903	0.01900	0.01900	0.01673	0.01661
90	12	1.42988	0.71901	0.01902	0.01902	0.01679	0.01679
	16	1.42988	0.71901	0.01902	0.01902	0.01681	0.01681
	8	1.35858	0.68972	0.04646	0.04647	0.13749	0.13746
100	12	1.35867	0.68936	0.04650	0.04650	0.13755	0.13755
	16	1.35868	0.68934	0.04651	0.04651	0.13756	0.13756
	8	0.36672	0.27844	0.44122	0.44111	0.32723	0.32732
140	12	0.36684	0.27817	0.44131	0.44131	0.32753	0.32753
	16	0.36686	0.27814	0.44132	0.44132	0.32754	0.32754
	8	−0.22329	0.03164	0.66997	0.66955	0	0
180	12	−0.22312	0.03191	0.66999	0.66998	0	0
	16	−0.22312	0.03194	0.67000	0.67000	0	0

12. The values that should be zero such as $(\sigma_{nM} - \sigma_{nI}), (\tau_{ntM} - \tau_{ntI}), (U_M - U_I), (V_M - V_I)$ are less than 10^{-5} along the entire boundary when $M = 12$. The present method is found to yield rapidly converging results and highly satisfied boundary conditions.

3.2. MAXIMUM STRESS $S_{j\max}$ APPEARING AT EACH INCLUSION

Figures 3–6 show examples of stress distributions $(\sigma_1, \sigma_n, \sigma_t, \tau_{nt}, \sigma_{eq})$ when three circular inclusions are subjected to $\sigma_x^\infty = 1, \sigma_y^\infty = 0$ in comparison with the results for a single inclusion. In Figures 3 and 4 the interface stresses along the outer boundary where the maximum stress appears are indicated; on the other hand, in Figures 5 and 6 the stresses along the central boundary are shown. Here, σ_1 is the principal stress determined from $(\sigma_n, \sigma_t, \tau_{nt})$, and σ_{eq} is the equivalent stress in the von Mieses sense.

Figures 7 and 8 illustrate results with various numbers of inclusions $N = 2, 3, \ldots, 8$. In these figures the normalized maximum principal stress $S_{j\max}$, which appears at each inclusion, is shown. Here $S_{j\max} = \sigma_{j\max}/\sigma_0, \sigma_{j\max}$ is the maximum principal stress and σ_0 is the maximum stress of a single inclusion.

Table 2. Maximum principal stress for the circular inclusions whose number $N = 2, 7, 8, \infty$. ($a/b = 1, S_{\max} = \sigma_{\max}/\sigma_0, \sigma_0 = \sigma_{\max}$ of a single inclusion, $\sigma_x^\infty = 1, \sigma_y^\infty = 0$ in Figure 1)

		Matrix											
E_I/E_M	a/d	0.0		0.0		0.2		0.4		0.6		0.8	
	N	(deg.)	σ_0	(deg.)	$S_{\max}$	(deg.)	$S_{\max}$	(deg.)	$S_{\max}$	(deg.)	$S_{\max}$	(deg.)	$S_{\max}$
0.0	2	90.0	3.000	90.0	1.000	89.7	0.976	88.0	0.926	85.9	0.890	84.2	0.874
			(3.000)		(1.000)		(0.976)		(0.926)		(0.890)		(0.874)
	7	90.0	3.000	90.0	1.000	89.6	0.964	87.7	0.896	85.4	0.847	83.9	0.822
			(3.000)		(1.000)		(0.964)		(0.896)		(0.847)		(0.822)
	8	90.0	3.000	90.0	1.000	89.6	0.964	87.7	0.895	85.4	0.845	83.9	0.820
	∞		3.000		1.000		0.961		0.885		0.831		0.806
			(3.000)		(1.000)		(0.961)		(0.886)		(0.832)		(0.806)
0.5	2	90.0	1.506	90.0	1.000	89.9	0.994	89.4	0.980	88.6	0.968	88.2	0.964
	7	90.0	1.506	90.0	1.000	89.9	0.991	89.3	0.969	88.3	0.948	87.5	0.932
	8	90.0	1.506	90.0	1.000	89.9	0.991	89.3	0.969	88.3	0.947	87.5	0.931
	∞		1.506		1.000		0.991		0.966		0.940		0.921
2.0	2	22.4, 157.6	1.215	22.4, 157.6	1.000	157.7	1.006	158.8	1.030	163.6	1.183	180.0	1.183
	7	22.4, 157.6	1.215	22.4, 157.6	1.000	157.7	1.015	158.7	1.062	163.8	1.155	180.0	1.330
	8	22.4, 157.6	1.215	22.4, 157.6	1.000	157.7	1.015	158.7	1.064	163.8	1.160	180.0	1.341
	∞		1.215		1.000		1.018		1.076		1.19		1.41
∞	2	21.8, 158.2	1.549	21.8, 158.2	1.000	158.4	1.017	160.3	1.083	166.3	1.602	180.0	1.737
	7	21.8, 158.2	1.549	21.8, 158.2	1.000	158.3	1.039	160.0	1.179	166.3	1.673	180.0	2.519
	8	21.8, 158.2	1.549	21.8, 158.2	1.000	158.3	1.040	160.0	1.182	166.3	1.677	180.0	2.610
	∞		1.549		1.000		1.047		1.221		1.70		3.2

Table 2 continued.

		Inclusion											
E_I/E_M	a/d	0.0		0.0		0.2		0.4		0.6		0.8	
	N	(deg.)	σ_0	(deg.)	$S_{\max}$	(deg.)	$S_{\max}$	(deg.)	$S_{\max}$	(deg.)	$S_{\max}$	(deg.)	$S_{\max}$
0.5	2	$0 \sim 180$	0.757	$0 \sim 180$	1.000	0.0	0.995	0.0	0.983	60.6	0.969	86.8	0.960
	7	$0 \sim 180$	0.757	$0 \sim 180$	1.000	0.0	0.992	0.0	0.973	0.0	0.950	75.7	0.931
	8	$0 \sim 180$	0.757	$0 \sim 180$	1.000	0.0	0.992	0.0	0.973	0.0	0.949	75.6	0.929
	∞		0.757		1.000		0.991		0.970		0.944		0.920
2.0	2	$0 \sim 180$	1.192	$0 \sim 180$	1.000	180.0	1.006	180.0	1.033	180.0	1.093	180.0	1.206
	7	$0 \sim 180$	1.192	$0 \sim 180$	1.000	180.0	1.015	180.0	1.065	180.0	1.169	180.0	1.355
	8	$0 \sim 180$	1.192	$0 \sim 180$	1.000	180.0	1.015	180.0	1.066	180.0	1.174	180.0	1.367
	∞		1.192		1.000		1.018		1.078		1.20		1.44
∞	2	$0 \sim 180$	1.475	$0 \sim 180$	1.000	180.0	1.017	180.0	1.092	180.0	1.650	180.0	1.823
	7	$0 \sim 180$	1.475	$0 \sim 180$	1.000	180.0	1.038	180.0	1.183	180.0	1.776	180.0	2.641
	8	$0 \sim 180$	1.475	$0 \sim 180$	1.000	180.0	1.039	180.0	1.189	180.0	1.781	180.0	2.736
	∞		1.475		1.000		1.046		1.228		1.82		3.4

Table 3. Maximum principal stress for the circular inclusions whose number $N = 2, 7, 8, \infty$. ($a/b = 1, S_{\max} = \sigma_{\max}/\sigma_0, \sigma_0 = \sigma_{\max}$ of a single inclusion, $\sigma_x^\infty = 0, \sigma_y^\infty = 1$ in Figure 1)

		Matrix											
E_I/E_M	a/d	0.0		0.0		0.2		0.4		0.6		0.8	
	N	(deg.)	σ_0	(deg.)	$S_{\max}$	(deg.)	$S_{\max}$	(deg.)	$S_{\max}$	(deg.)	$S_{\max}$	(deg.)	$S_{\max}$
0.0	2	0.0, 180.0	3.000	0.0, 180.0	1.000	0.0	1.001	0.0	1.011	180.0	1.039	180.0	1.345
			(3.000)		(1.000)		(1.001)		(1.011)		(1.039)		(1.345)
	7	0.0, 180.0	3.000	0.0, 180.0	1.000	0.0	1.001	0.0	1.022	180.0	1.137	180.0	1.703
			(3.000)		(1.000)		(1.001)		(1.022)		(1.137)		(1.703)
	8	0.0, 180.0	3.000	0.0, 180.0	1.000	0.0	1.001	0.0	1.023	180.0	1.142	180.0	1.726
	∞		3.000		1.000		1.002		1.075		1.182		1.918
			(3.000)		(1.000)		(1.002)		(1.075)		(1.182)		(1.918)
0.5	2	0.0, 180.0	1.506	0.0, 180.0	1.000	0.0	1.000	0.0	1.003	163.6	1.017	180.0	1.095
	7	0.0, 180.0	1.506	0.0, 180.0	1.000	0.0	1.001	0.0	1.007	163.6	1.029	180.0	1.125
	8	0.0, 180.0	1.506	0.0, 180.0	1.000	0.0	1.001	0.0	1.007	163.6	1.030	180.0	1.126
	∞		1.506		1.000		1.001		1.007		1.037		1.133
2.0	2	67.7, 112.3	1.215	67.7, 112.3	1.000	67.6	0.999	67.5	0.997	67.2	0.993	66.6	0.986
	7	67.7, 112.3	1.215	67.7, 112.3	1.000	67.6	0.999	67.5	0.996	67.1	0.991	66.6	0.983
	8	67.7, 112.3	1.215	67.7, 112.3	1.000	67.6	0.999	65.7	0.996	67.1	0.991	66.6	0.983
	∞		1.215		1.000		0.999		0.996		0.991		0.983
∞	2	67.9, 112.1	1.549	67.9, 112.1	1.000	68.2	1.000	68.3	1.000	113.5	1.004	68.7	0.998
	7	67.9, 112.1	1.549	67.9, 112.1	1.000	68.2	1.000	68.3	1.002	113.5	0.998	69.6	1.027
	8	67.9, 112.1	1.549	67.9, 112.1	1.000	68.2	1.000	68.3	1.002	113.5	0.998	69.6	1.030
	∞		1.549		1.000		1.000		1.002		0.998		1.051

Table 3 continued.

		Inclusion											
E_I/E_M	a/d	0.0		0.0		0.2		0.4		0.6		0.8	
	N	(deg.)	σ_0	(deg.)	S_{max}	(deg.)	S_{max}	(deg.)	S_{max}	(deg.)	S_{max}	(deg.)	S_{max}
0.5	2	$0 \sim 180$	0.757	$0 \sim 180$	1.000	125.0	1.001	132.5	1.008	157.1	1.029	180.0	1.114
	7	$0 \sim 180$	0.757	$0 \sim 180$	1.000	90.0	1.004	90.0	1.018	142.9	1.052	180.0	1.159
	8	$0 \sim 180$	0.757	$0 \sim 180$	1.000	90.0	1.004	91.0	1.019	142.9	1.053	180.0	1.161
	∞		0.757		1.000		1.004		1.026		1.060		1.175
2.0	2	$0 \sim 180$	1.192	$0 \sim 180$	1.000	180.0	1.006	0.0	0.998	0.0	0.998	0.0	0.999
	7	$0 \sim 180$	1.192	$0 \sim 180$	1.000	180.0	1.015	0.0	0.998	0.0	0.997	0.0	0.997
	8	$0 \sim 180$	1.192	$0 \sim 180$	1.000	180.0	1.015	0.0	0.998	0.0	0.997	0.0	0.997
	∞		1.192		1.000		1.018		0.998		0.997		0.997
∞	2	$0 \sim 180$	1.475	$0 \sim 180$	1.000	0.0	1.000	0.0	1.005	0.0	1.110	0.0	1.057
	7	$0 \sim 180$	1.475	$0 \sim 180$	1.000	0.0	0.999	0.0	1.006	0.0	1.371	0.0	1.091
	8	$0 \sim 180$	1.475	$0 \sim 180$	1.000	0.0	0.999	0.0	1.006	0.0	1.380	0.0	1.093
	∞		1.475		1.000		0.999		1.006		1.443		1.107

Table 4. Maximum principal stress and maximum normal stress of the matrix when $N \to \infty$. ($S_{\max} = \sigma_{\max}/\sigma_0, S_{n\max} = \sigma_{n\max}/\sigma_{n0}, \sigma_x^\infty = 1, \sigma_y^\infty = 0$ in Figure 1)

$\rho/a = (b/a)^2$	a/d	0.0	0.0	0.2	0.4	0.6	0.8
	E_I/E_M	σ_0 σ_{n0}	$S_{\max}$ $S_{n\max}$	$S_{\max}$ $S_{n\max}$	$S_{\max}$ $S_{n\max}$	$S_{\max}$ $S_{n\max}$	$S_{\max}$ $S_{n\max}$
1.0	0.0	3.000	1.000	0.961	0.885	0.831	0.806
		0.000	0.000	0.000	0.000	0.000	0.000
	0.5	1.506	1.000	0.990	0.965	0.940	0.921
		0.757	1.000	0.991	0.970	0.944	0.917
	2.0	1.215	1.000	1.018	1.076	1.19	1.41
		1.192	1.000	1.018	1.078	1.21	1.44
	∞	1.549	1.000	1.047	1.224	1.70	3.5
		1.478	1.000	1.046	1.229	1.75	3.7
0.8	0.0	2.789	1.000	0.966	0.895	0.844	0.815
		0.000	0.000	0.000	0.000	0.000	0.000
	0.5	1.477	1.000	0.991	0.968	0.943	0.894
		0.741	1.000	0.993	0.974	0.950	0.925
	2.0	1.235	1.000	1.016	1.070	1.179	1.392
		1.213	1.000	1.016	1.071	1.189	1.417
	∞	1.612	1.000	1.042	1.205	1.66	3.3
		1.542	1.000	1.042	1.209	1.69	3.5
0.6	0.0	2.549	1.000	0.973	0.913	0.861	0.831
		0.000	0.000	0.000	0.000	0.000	0.000
	0.5	1.439	1.000	0.992	0.972	0.948	0.863
		0.721	1.000	0.993	0.977	0.957	0.879
	2.0	1.263	1.000	1.015	1.063	1.163	1.364
		1.241	1.000	1.014	1.063	1.173	1.389
	∞	1.705	1.000	1.039	1.188	1.59	3.1
		1.636	1.000	1.039	1.189	1.61	3.2
0.4	0.0	2.265	1.000	0.979	0.930	0.883	0.853
		0.000	0.000	0.000	0.000	0.000	0.000
	0.5	1.387	1.000	0.993	0.977	0.955	0.935
		0.693	1.000	0.995	0.982	0.966	0.949
	2.0	1.307	1.000	1.012	1.053	1.141	1.322
		1.284	1.000	1.012	1.053	1.144	1.346
	∞	1.864	1.000	1.034	1.165	1.519	2.79
		1.794	1.000	1.034	1.165	1.527	2.90
0.2	0.0	1.894	1.000	0.939	0.810	0.691	0.608
		0.000	0.000	0.000	0.000	0.000	0.000
	0.5	1.303	1.000	0.996	0.985	0.967	0.949
		0.649	1.000	0.996	0.988	0.977	0.966
	2.0	1.390	1.000	1.009	1.040	1.107	1.249
		1.367	1.000	1.009	1.040	1.107	1.270
	∞	2.228	1.000	1.040	1.145	1.421	2.420
		2.151	1.000	1.028	1.135	1.420	2.463

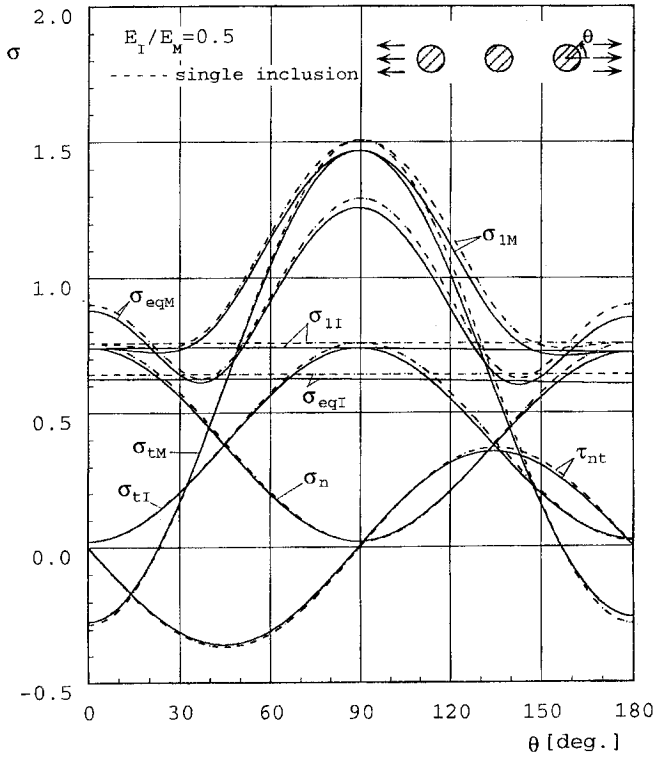

Figure 4. Stress distribution along the outer boundary for three circular inclusions. ($N = 3, a/b = 1, a/d = 0.4, \sigma_x^\infty = 1, \sigma_y^\infty = 0, E_I/E_M = 0.5$ in Figure 1)

When the tensile direction is parallel to the row axis ($\sigma_x^\infty = 1, \sigma_y^\infty = 0$), the maximum stress $S_{\max}$ appears at the outermost inclusion for $E_I/E_M < 1$ and it appears at the central inclusion for $E_I/E_M > 1$. On the other hand, when the tensile direction is perpendicular to the row axis ($\sigma_x^\infty = 0, \sigma_y^\infty = 1$), the maximum stress $S_{\max}$ appears at the outermost inclusion for $E_I/E_M > 1$ and it appears at the central inclusion for $E_I/E_M < 1$. The limiting values for an infinite number N can be obtained by extrapolation using the linearity between $1/N$ and $S_{\max}$ (See Section 3.3).

3.3. MAXIMUM STRESS $S_{\max}$ VS N RELATION

Figure 9 shows relationships between the maximum stresses $S_{\max}$, which is the maximum value among $S_{j\max}$, and the reciprocal of the number of inclusions N when $\sigma_x^\infty = 1, \sigma_y^\infty = 0, E_I/E_M = 0.5$. Figure 10 also shows relationships between the maximum stresses $S_{\max}$ and $1/(N - 0.5)$ when $\sigma_x^\infty = 0, \sigma_y^\infty = 1, E_I/E_M = 0.5$ and $a/d = 0.2, 0.4, 0.6, 0.8$. Isida and Igawa have shown a linear relation between $1/N$ and $S_{\max}$ when a row of elliptical holes are subjected to $\sigma_x^\infty = 1, \sigma_y^\infty = 0$, and a linear relation between $1/(N - 0.5)$ and $S_{\max}$ when a row of elliptical holes are subjected to under $\sigma_x^\infty = 0, \sigma_y^\infty = 1$ [5]. Figures 9 and 10 show a similar relation between $S_{\max}$ and N in a row of elliptical inclusions.

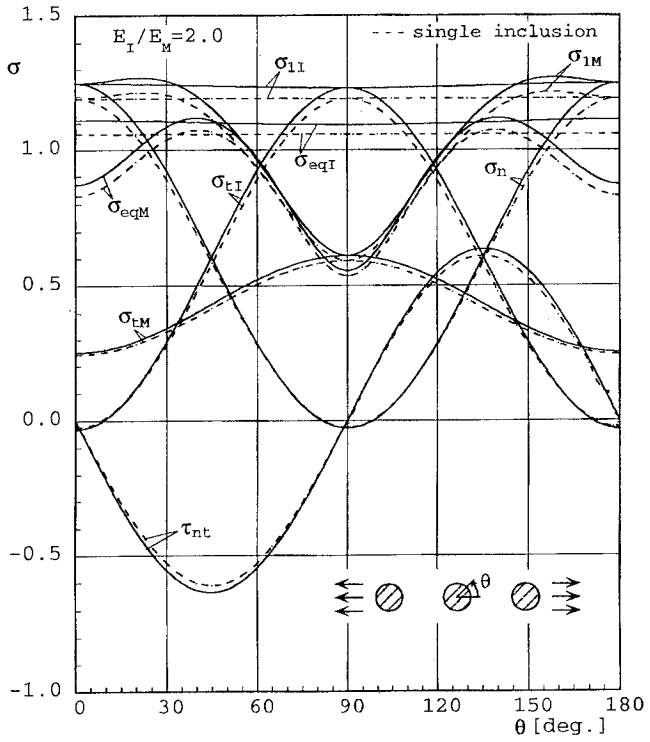

Figure 5. Stress distribution along the central boundary for three circular inclusions. ($N = 3, a/b = 1, a/d = 0.4, \sigma_x^\infty = 1, \sigma_y^\infty = 0, E_I/E_M = 2.0$ in Figure 1)

3.4. MAXIMUM PRINCIPAL STRESS $S_{\max}$ AND MAXIMUM NORMAL STRESS $S_{n\max}$ IN A ROW OF ELLIPTICAL INCLUSIONS

Tables 2 and 3 show the maximum values and position of $S_{\max}$. When $E_I/E_M = 0$, Isida–Igawa's results [5] for circular holes coincide with the present results to the last digit as shown. In these tables the values of normalized maximum normal stress $S_{n\max}$ are also shown because they may cause separation of the interface. Here $S_{n\max} = \sigma_{n\max}/\sigma_{n0}, \sigma_{n\max}$ is the maximum normal stress among the inclusions and σ_{n0} is the maximum normal stress of a single inclusion. In Tables 4–7, $S_{\max}$ and $S_{n\max}$ for $N \to \infty$ are shown, which are obtained by extrapolation from the results of $N = 6, 7, 8$. Here, ρ is the root radius of ellipse, and the results are indicated while varying the shape parameter of ellipse $(b/a)^2 = \rho/a$.

4. Conclusions

In this paper, the interaction effect of a row of elliptical inclusions, as shown in Figure 1, is discussed using the singular integral equations of the body force method. The interface stresses are shown graphically and the maximum stresses are tabulated while varying the shape, size, and elastic constants of inclusions. The conclusions are summarized as follows:

(1) The interaction problem between elliptical and ellipsoidal inclusions was formulated in terms of singular integral equations with the Cauchy-type and logarithmic-type singularity. To formulate the problem the body force method was applied where the Green's functions were used as the fundamental solutions.

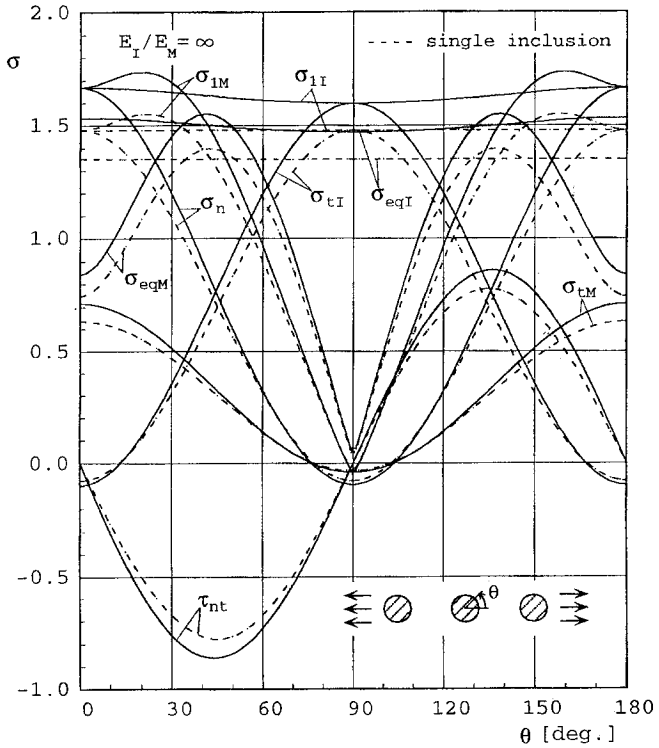

Figure 6. Stress distribution along the central boundary for three circular inclusions. ($N = 3, a/b = 1, a/d = 0.4, \sigma_x^\infty = 1, \sigma_y^\infty = 0, E_I/E_M = \infty$ in Figure 1)

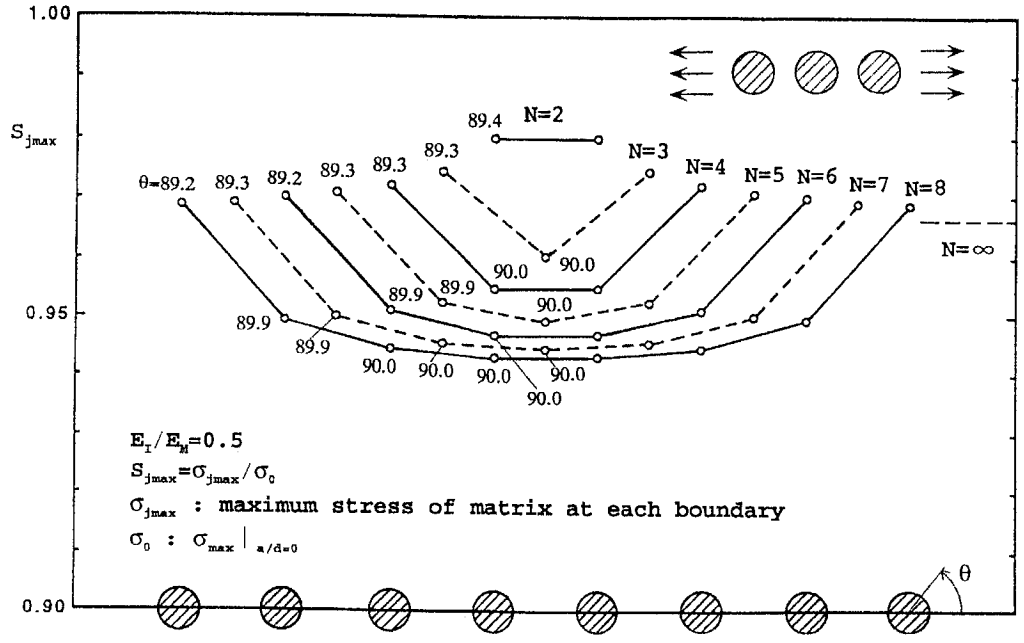

Figure 7. Variation of normalized maximum principal stress at each inclusion $S_{j\max}$ when the number of inclusions $N = 2, 3, \ldots, 8$. ($a/b = 1, a/d = 0.4, \sigma_x^\infty = 1, \sigma_y^\infty = 0, E_I/E_M = 0.5$ in Figure 1)

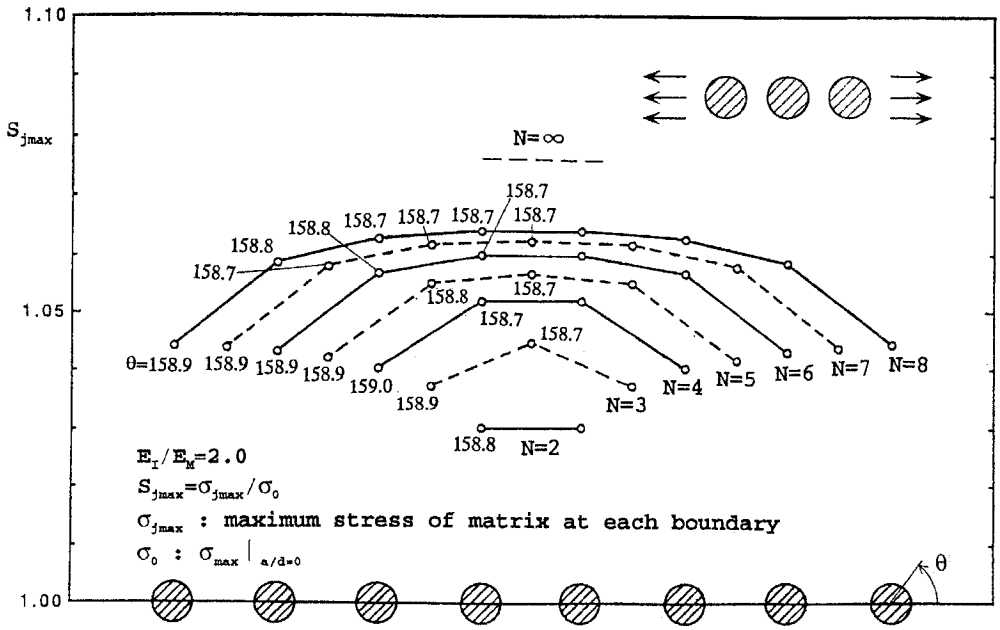

Figure 8. Variation of normalized maximum principal stress at each inclusion $S_{j\max}$ when the number of inclusions $N = 2, 3, \ldots, 8$. ($a/b = 1, a/d = 0.4, \sigma_x^\infty = 1, \sigma_y^\infty = 0, E_I/E_M = 2.0$ in Figure 1)

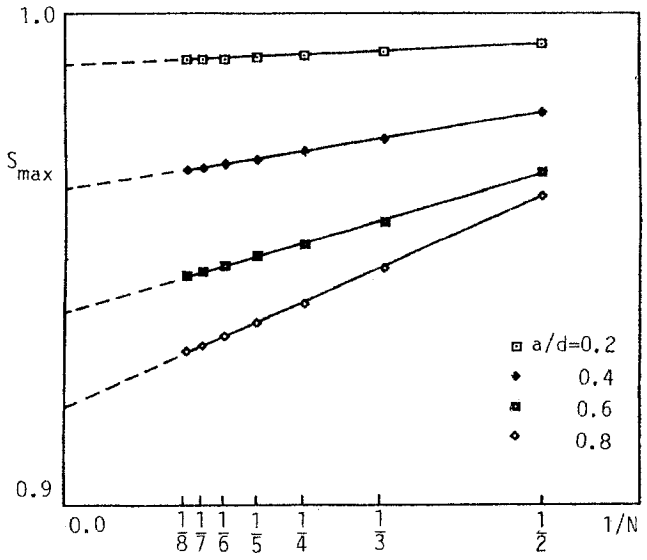

Figure 9. Relationship between $S_{\max}$ and $1/N$. ($a/b = 1, \sigma_x^\infty = 1, \sigma_y^\infty = 0, E_I/E_M = 0.5$ in Figure 1)

Table 5. Maximum principal stress of the inclusion when $N \to \infty$. ($S_{max} = \sigma_{max}/\sigma_0, \sigma_x^\infty = 1, \sigma_y^\infty = 0$ in Figure 1)

$\rho/a = (b/a)^2$	a/d	0.0	0.0	0.2	0.4	0.6	0.8
	E_I/E_M	σ_0	S_{max}	S_{max}	S_{max}	S_{max}	S_{max}
1.0	0.0	0.000	0.000	0.000	0.000	0.000	0.000
	0.5	0.757	1.000	0.991	0.970	0.944	0.920
	2.0	1.192	1.000	1.018	1.078	1.20	1.44
	∞	1.478	1.000	1.046	1.228	1.82	3.4
0.8	0.0	0.000	0.000	0.000	0.000	0.000	0.000
	0.5	0.741	1.000	0.993	0.974	0.950	0.926
	2.0	1.213	1.000	1.016	1.071	1.189	1.417
	∞	1.542	1.000	1.042	1.209	1.69	3.51
0.6	0.0	0.000	0.000	0.000	0.000	0.000	0.000
	0.5	0.721	1.000	0.993	0.977	0.957	0.879
	2.0	1.241	1.000	1.014	1.063	1.169	1.389
	∞	1.636	1.000	1.039	1.189	1.61	3.24
0.4	0.0	0.000	0.000	0.000	0.000	0.000	0.000
	0.5	0.693	1.000	0.995	0.982	0.966	0.949
	2.0	1.284	1.000	1.012	1.053	1.144	1.346
	∞	1.794	1.000	1.034	1.165	1.527	2.909
0.2	0.0	0.000	0.000	0.000	0.000	0.000	0.000
	0.5	0.649	1.000	0.997	0.988	0.977	0.966
	2.0	1.367	1.000	1.009	1.040	1.107	1.270
	∞	2.151	1.000	1.048	1.175	1.481	4.265

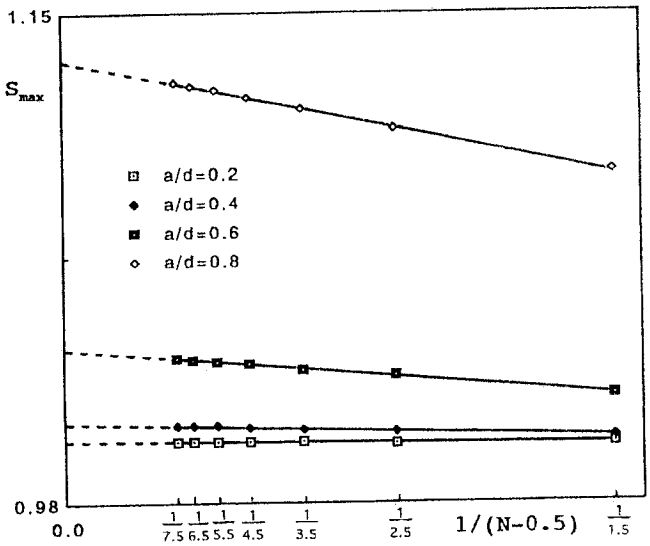

Figure 10. Relationship between S_{max} and $1/(N-0.5)$. ($a/b = 1, \sigma_x^\infty = 0, \sigma_y^\infty = 1, E_I/E_M = 0.5$ in Figure 1)

Table 6. Maximum principal stress and maximum normal stress of the matrix when $N \to \infty$. ($S_{\max} = \sigma_{\max}/\sigma_0, S_{n\max} = \sigma_{n\max}/\sigma_{n0}, \sigma_x^\infty = 0, \sigma_y^\infty = 1$ in Figure 1)

$\rho/a = (b/a)^2$	a/d	0.0	0.0	0.2	0.4	0.6	0.8
	E_I/E_M	σ_0 σ_{n0}	$S_{\max}$ $S_{n\max}$	$S_{\max}$ $S_{n\max}$	$S_{\max}$ $S_{n\max}$	$S_{\max}$ $S_{n\max}$	$S_{\max}$ $S_{n\max}$
1.0	0.0	3.000	1.000	1.002	1.075	1.182	1.918
		0.000	0.000	0.000	0.000	0.000	0.000
	0.5	1.506	1.000	1.001	1.010	1.037	1.133
		0.757	1.000	0.990	0.885	0.831	0.806
	2.0	1.215	1.000	0.999	0.996	0.991	0.983
		1.192	1.000	1.000	0.978	0.982	0.965
	∞	1.549	1.000	1.000	1.002	0.998	1.051
		1.478	1.000	1.047	1.221	1.70	3.2
0.8	0.0	3.236	1.000	1.003	1.035	1.170	1.821
		0.000	0.000	0.000	0.000	0.000	0.000
	0.5	1.535	1.000	1.001	1.007	1.028	1.117
		0.773	1.000	1.003	1.019	1.051	1.106
	2.0	1.196	1.000	0.999	0.997	0.992	0.986
		1.173	1.000	0.999	0.994	0.984	0.969
	∞	1.494	1.000	0.987	0.967	0.943	0.933
		1.420	1.000	0.997	0.969	0.972	0.948
0.6	0.0	3.582	1.000	1.006	1.039	1.162	1.732
		0.000	0.000	0.000	0.000	0.000	0.000
	0.5	1.571	1.000	1.001	1.006	1.023	1.095
		0.794	1.000	1.003	1.015	1.042	1.089
	2.0	1.174	1.000	0.999	0.997	0.994	0.990
		1.150	1.000	0.999	0.994	0.987	0.974
	∞	1.433	1.000	0.991	0.979	0.958	0.946
		1.355	1.000	0.998	0.990	0.977	0.956
0.4	0.0	4.162	1.000	1.008	1.045	1.158	1.637
		0.000	0.000	0.000	0.000	0.000	0.000
	0.5	1.619	1.000	1.001	1.005	1.016	1.071
		0.821	1.000	1.003	1.012	1.032	1.076
	2.0	1.147	1.000	0.999	0.998	0.996	0.994
		1.122	1.000	0.999	0.996	0.991	0.980
	∞	1.365	1.000	0.993	0.983	0.965	0.958
		1.278	1.000	0.998	0.992	0.974	0.965
0.2	0.0	5.472	1.000	1.017	1.075	1.028	1.044
		0.000	0.000	0.000	0.000	0.000	0.000
	0.5	1.692	1.000	1.001	1.004	1.013	1.044
		0.863	1.000	1.002	1.009	1.022	1.047
	2.0	1.110	1.000	1.000	0.999	0.998	0.997
		1.084	1.000	1.000	0.992	0.994	0.988
	∞	1.289	1.000	0.995	0.988	0.981	0.973
		1.176	1.000	0.999	0.996	0.989	0.978

Table 7. Maximum principal stress of the inclusion when $N \to \infty$. ($S_{max} = \sigma_{max}/\sigma_0, \sigma_x^\infty = 0, \sigma_y^\infty = 1$ in Figure 1)

$\rho/a = (b/a)^2$	a/d	0.0	0.0	0.2	0.4	0.6	0.8
	E_I/E_M	σ_0	S_{max}	S_{max}	S_{max}	S_{max}	S_{max}
1.0	0.0	0.000	0.000	0.000	0.000	0.000	0.000
	0.5	0.757	1.000	1.004	1.026	1.060	1.175
	2.0	1.192	1.000	0.999	0.998	0.997	0.997
	∞	1.475	1.000	0.999	1.006	1.443	1.107
0.8	0.0	0.000	0.000	0.000	0.000	0.000	0.000
	0.5	0.773	1.000	1.004	1.019	1.053	1.155
	2.0	1.173	1.000	0.999	0.997	0.996	0.996
	∞	1.420	1.000	1.109	1.299	1.406	1.591
0.6	0.0	0.000	0.000	0.000	0.000	0.000	0.000
	0.5	0.793	1.000	1.004	1.016	1.045	1.131
	2.0	1.150	1.000	0.999	0.997	0.996	0.995
	∞	1.355	1.000	1.081	1.222	1.420	1.854
0.4	0.0	0.000	0.000	0.000	0.000	0.000	0.000
	0.5	0.821	1.000	1.003	1.012	1.035	1.101
	2.0	1.122	1.000	0.999	0.998	0.996	0.995
	∞	1.278	1.000	1.086	1.233	1.476	1.996
0.2	0.0	0.000	0.000	0.000	0.000	0.000	0.000
	0.5	0.863	1.000	1.002	1.009	1.024	1.068
	2.0	1.084	1.000	0.999	0.998	0.997	0.995
	∞	1.176	1.000	1.126	1.319	1.658	2.481

(2) In the present analysis, the unknown functions of the body force densities were approximated by a linear combination of the fundamental density functions and weight functions. The boundary conditions were found to be highly satisfied by the present method along the entire boundary.

(3) When the tensile direction is parallel to the row axis ($\sigma_x^\infty = 1, \sigma_y^\infty = 0$), the maximum stress S_{max} appears at the outermost inclusion for $E_I/E_M < 1$ and at the central inclusion for $E_I/E_M > 1$.

(4) When the tensile direction is perpendicular to the row axis ($\sigma_x^\infty = 0, \sigma_y^\infty = 1$), the maximum stress S_{max} appears at the outermost inclusion for $E_I/E_M > 1$ and at the central inclusion for $E_I/E_M > 1$.

(5) A linear relationship was found between $1/N$ and S_{max} when a row of elliptical inclusions are subjected to $\sigma_x^\infty = 1, \sigma_y^\infty = 0$, and between $1/(N\text{–}0.5)$ and S_{max} when a row of elliptical inclusions are subjected to under $\sigma_x^\infty = 0, \sigma_y^\infty = 1$, where N is the number of inclusions. Using these relationships, the limiting values of S_{max} were obtained for $N \to \infty$.

The authors wish to express their gratitude to the reviewer's many useful discussions and suggestions.

References

1. L.H. Donnel, Stress concentrations due to elliptical discontinuities in plates under edge forces. Ann. Vol. T. Von Karman, Calif. Inst. Tech. (1941) 293–309.
2. S. Shioya, Tension of infinite thin plate containing two elliptical inclusions. *Transactions of the Japan Society of Mechanical Engineers* 36 (1970) 886–897.
3. J.D. Eshelby, The determination of the elastic field of an ellipsoidal inclusion and related problems. *Proc. Royal Soc.*, A. 241 (1957) 376–396.
4. J.D. Eshelby, The elastic field outside an ellipsoidal inclusion. *Proc. Royal Soc.*, A. 252 (1959) 561–569.
5. M. Isida and H. Igawa, Some asymptotic behavior and formulate of stress intensity factors for collinear and parallel cracks under various loadings. *International Journal of Fracture* 65 (1994) 247–259.
6. N.A. Noda and T. Matsuo, Singular integral equation method in the analysis of interaction between crack and defects. *Fracture Mechanics: 25th Volume*, ASTM STP 1220, (ed. Erdogan, F.), American Society for Testing and Materials, (1995) 591–605.
7. N.A. Noda and T. Matsuo, Singular integral equation method in optimization stress-relieving hole: A new approach based on the body force method. *International Journal of Fracture* 70 (1995) 147–165.
8. H. Nisitani, The two-dimensional stress problem solved using an electric digital computer. *Journal of the Japan Society of Mechanical Engineers* 70 (1967) 627–632. [*Bulletin of Japan Society of Mechanical Engineers* 11 (1968) 14–23.]
9. H. Nisitani, Solution of Notch Problems by Body Force Method, Stress Analysis of Notched Problem (ed. Sih, G.C.), Noordhoff International Publication, Leyden, 5 (1974) 1–68.
10. H. Nisitani and D.H. Chen, *The Body Force Method* (Taisekiryokuho in Japanese), Baifukan Publication, Tokyo (1987).